

# MotionDeltaCNN: Sparse CNN Inference of Frame Differences in Moving Camera Videos

Mathias Parger<sup>1</sup> Chengcheng Tang<sup>2</sup> Thomas Neff<sup>1</sup> Christopher D. Twigg<sup>2</sup> Cem Keskin<sup>2</sup>  
Robert Wang<sup>2</sup> Markus Steinberger<sup>1</sup>

<sup>1</sup>Graz University of Technology, <sup>2</sup>Meta Reality Labs

<sup>1</sup>{mathias.parger, steinberger}@icg.tugraz.at

<sup>2</sup>{chengcheng.tang, cdtwigg, cemkeskin, rywang}@fb.com

## Abstract

*Convolutional neural network inference on video input is computationally expensive and has high memory bandwidth requirements. Recently, researchers managed to reduce the cost of processing upcoming frames by only processing pixels that changed significantly. Using sparse convolutions, the sparsity of frame differences can be translated to speedups on current inference devices. However, previous work was relying on static cameras. Moving cameras add new challenges in how to fuse newly unveiled image regions with already processed regions efficiently to minimize the update rate - without increasing memory overhead and without knowing the camera extrinsics of future frames. In this work, we propose MotionDeltaCNN, a CNN framework that supports moving cameras and variable resolution input. We propose a spherical buffer which enables seamless fusion of newly unveiled regions and previously processed regions - without increasing the memory footprint. Our evaluation shows that we outperform previous work by up to 90% by explicitly adding support for moving camera input.*

## 1. Introduction

The rise of convolutional neural networks (CNN) for image understanding tasks took off with porting the training process onto GPUs [17]. While the concept of CNNs existed long before that, training them was very time consuming and therefore impracticable. Implementing the computationally heavy kernels on GPUs accelerated the training procedure by orders of magnitude, untying the knot to great machine learning progress that followed soon after.

Since then, incremental hardware improvements, as well as special hardware designs for inference, enable CNN inference even on mobile devices only a decade later. However, real-time inference is still highly power-consuming and processing videos or live streams is often not possible

on mobile devices due to hardware and thermal limitations. Many researchers are working on different approaches to tackle the high compute demands of CNNs. Famous methods include pruning [13, 18], quantization [15, 21, 23], specialized hardware [4, 5, 12] or network optimization [29, 31] to name a few. While these improvements reduce inference cost, real-time inference still remains expensive in terms of hardware requirements and energy-consumption. Yet, video input offers unique ways for performance optimization due to the temporal similarity between frames [24, 28]. One common approach to exploit this similarity is to use large, slow networks to create accurate predictions at key frames that are updated using small, fast networks at intermediate frames [8, 11, 16, 19, 20, 32, 33]. The downside of these approaches is that they can not be applied to existing CNN architectures, but require special designs and training processes. Also, for best results, the intermediate frames should not differ greatly from the base frame that was inferred with the precise model. Sparse convolutions, on the other hand, do not require special architectures and can be used with existing models. With sparse convolutions, the large network can be accelerated to run at the speed of the smaller network with marginal impact on the prediction accuracy [25, 26].

The linearity of convolutions enables the accumulation of updates over consecutive frames. After processing the first frame densely, upcoming frames can be processed using the difference between the current and the previous frame, the *Delta*, as the network input. Assuming a static camera scenario, this results in large image regions with no frame-to-frame difference. Static elements like background or stationary objects do not require updates after the initial frame, resulting in a high update sparsity. Researchers exploited this sparsity in previous work to reduce the number of FLOPs required for CNN inference [1, 3, 7, 10, 25], but were mostly unable to accelerate inference in practice. With the recent progress in DeltaCNN [26], theoretical FLOP reductions were translated into practical speedups on GPUs, using a

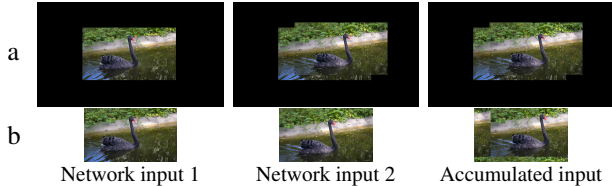


Figure 1. Illustration of different approaches to support moving camera input. The naïve approach (a) is to embed the input onto a larger image and only overwrite pixels that are covered in the next frame. This approach comes with large overhead for storing the additional pixels of the embedded frame and for checking all pixels for updates. MotionDeltaCNN (b) uses original shape buffers and feature maps - avoiding the memory overhead and reducing the number of pixels that have to be checked for updates.

custom sparse CNN implementation to exploit sparsity in all layers of the CNN.

Although DeltaCNN shows speedups for various use cases and datasets, it, as well as all previous work, is designed around static camera input. Even with only small frame to frame camera motion, large parts of the input — probably even the entire image — require reprocessing since pixels do not align with their previous values. An obvious solution to increase update sparsity would be to correct the camera offset between frames. With image warping, consecutive frames can be aligned to achieve higher consistency of pixels. Fortunately, camera extrinsics needed for alignment are often available for free on mobile devices from inertial measurement units in mobile phones or SLAM in VR headsets. However, when aligning two images from different perspectives, parts of the image do not overlap and extend outside the field of view covered by the initial frame - thereby also going out of bounds of the buffers storing the previous results which are essential for sparse CNN inference. One way to solve this issue is to embed inputs in a larger frame by padding the input image and drawing updates on top of it. The downside of this approach is that padded input images increase the size of all feature maps significantly - adding overhead for checking all empty pixels for updates (see Figure 1 a vs. b). At the same time, large feature maps result in large storage overhead for buffers while smaller paddings limit the range which can be stabilized without exceeding buffer borders. If the direction of camera motion is known, the overhead can be reduced by only padding towards that direction, but this information is not available in the general use case.

In this work, we propose MotionDeltaCNN, a sparse CNN inference framework that allows for panning camera input with only marginal memory overhead. MotionDeltaCNN supports theoretically infinite camera motion while achieving a high reuse of previously computed results. Compared to previous work, we achieve up to 90% higher frame rates

in videos with moving cameras. We hope that our work helps to pave the way for using CNNs on low-power devices, such as surveillance cameras, smartphones or virtual reality devices. Our main contributions are:

- We design a two-dimensional ring buffer, a *spherical buffer*, with wrapped coordinates. Our buffer allows partial growth, reset and initialization of new tiles while keeping previously processed regions intact.
- We modify convolutional layers for seamless integration of newly unveiled neighbor regions without the need of reprocessing before seen pixels.
- We show how MotionDeltaCNN can also be used for speeding up applications with static cameras when only parts of the image require processing.

## 2. Related Work

The idea of only processing updated pixels in a convolutional layer has been proposed in various ways, with *Recurrent Residual Module (RRM)* [25] being the first work to apply this concept to videos. RRM uses the difference between current and previous input, the *Delta*, as input to convolutional layers. RRM shows that FLOPs can be reduced significantly compared to dense inference. However, RRM evaluates only theoretical FLOP reductions where every (close to) zero-valued feature in the feature map is considered a sparse feature that can be skipped to achieve a speedup. In practice, skipping values individually is infeasible on most inference hardware like GPUs due to their single instruction, multiple data (SIMD) design. Furthermore, RRM only processes convolutional layers on sparse Delta input. All remaining layers are processed on the full, dense feature maps and therefore require expensive value-conversions before and after each convolutional layer.

*Skip-Convolution* [10] and *CBInfer* [3] improve the concept of RRM using a per-pixel sparse mask instead of per-value. Similar to RRM, CBInfer uses a threshold to truncate insignificant updates in the input feature map. This threshold can be tuned for each layer for maximum sparsity while keeping the accuracy above a desired level. In contrast, Skip-Convolution decides per *output* pixel whether an update is required or can be skipped. In both cases, only the convolutional layers (and pooling layers in case of CBInfer) are processed sparsely, requiring expensive conversions between dense and sparse features before and after each of these layers, leaving large performance potential unused.

*DeltaCNN* [26] propagates sparse Delta features end-to-end using a sparse Delta feature map together with an update mask. This greatly reduces the memory bandwidth compared to previous work. Propagating sparse updates end-to-end eliminates the necessity of converting the feature maps from dense accumulated values to sparse Deltas, and it speeds up



Figure 2. The main concepts of MotionDeltaCNN. We align frame 2 (F2) with frame 1 (F1) using homography matrices. For the intersecting region, we propagate only the frame-to-frame differences (Delta). The newly uncovered regions are propagated directly (*Aligned Delta*). The regions in which the buffers store the uncovered regions are reset to zero before processing the current Delta input. After convolving frame 2, we add the bias to all previously unseen regions, and accumulate the result onto our spherical buffer using the offset coordinates for the current frame.

other layers bottlenecked by memory bandwidth like activation, batch normalization, upsampling, etc. Using a custom CUDA implementation, DeltaCNN outperforms cuDNN and CBInfer many times on video input. However, DeltaCNN, as well as all other previous work, assumes a static camera input. Even single pixel camera motion between two frames can result in nearly dense updates when the image contains high frequency features.

*Event Neural Networks* show that computational savings are strongly impacted by the intensity of camera motion [7]. With slightly shaking cameras, theoretical FLOP savings were reduced by 40% compared to static camera videos, while moving cameras reduce them by 60%. Depending on the distribution of the pixel updates, the impact on real hardware is likely even higher.

*Incremental Sparse Convolution* uses sparse convolutions to incrementally update 3D segmentation masks online [22]. They solve a similar problem of reusing results from previously segmented regions, while allowing for new regions to be attached on the fly. Due to their reliance on non-dilating 3D convolutions [9], attaching new regions leads to artifacts along the region borders. We solve this issue using a standard, dilating convolution and by processing all outputs that are affected by the current input.

We propose MotionDeltaCNN: building upon DeltaCNN, we design and implement a sparse inference extension that supports moving cameras. Compared to DeltaCNN, we add the support for variable resolution inputs, spherical buffers, dynamic buffer allocation & initialization and padded convolutions for seamless attachment of newly unveiled regions.

### 3. Method

MotionDeltaCNN tackles the problems of panning camera input for accumulative sparse CNN inference by relying on the following concepts:

- **Frame alignment:** The current frame is aligned with the initial frame of the sequence to maximize the overlap of consistent features (see Figure 2 *Aligned Delta*).
- **Spherical buffers:** We use wrapped buffer offset coordinates in all non-linear layers to align them with the input (see Figure 2 *Accumulated Result*).
- **Dynamic initialization:** When a new region is first unveiled due to camera motion, MotionDeltaCNN adds biases onto the feature maps on the fly to all newly unveiled pixels to allow for seamless integration with previously processed pixels (see Figure 2 *Bias*).
- **Padded convolutions:** We add additional padding to convolutional layers to process all pixels that are affected by the kernel. These *dilated* pixels are stored in truncated values buffers to enable seamless connection of potentially unveiled neighbor regions in upcoming frames (see Figure 3).

#### 3.1. Background

For a better understanding of our contributions, we first summarize the core concept of the original DeltaCNN. DeltaCNN accelerates CNN inference by processing only the first frame densely and applying sparse updates for changed pixels in upcoming frames. The updates are calculated by subtracting the previously processed input from the current input. In this process, insignificant updates (*i.e.*, pixels with a maximum norm below a threshold) can be truncated to increase the sparsity of the Delta features - reducing both FLOPs and memory bandwidth during inference, as only non-zero updates require processing. Non-linear layers like activation and pooling layers cannot be processed on Delta input directly, as they depend on the "full" values. Because of that, every non-linear layer requires its own buffer, the *accumulated values buffer*, to save the state at its stage in the network and to accumulate incoming updates in the following frames. The buffers contain the full, dense state of the feature map of the previous frame, including biases from previous layers. Thus, biases may not be used anymore after the first frame, as they are already stored in the buffers. Convolutions with kernel sizes larger than 1x1 pixels dilate the updates across the feature map. A single pixel update in the center of the feature map might span over the entire feature map few convolutional layers later. This can lead to nearly dense updates for the larger part of the network. DeltaCNN solves this by truncating insignificant updates not only on the input image, but at every activation layer. To avoid accumulating errors indefinitely, the truncated values are accumulated in a dedicated *truncated values buffer*. Once an accumulated, truncated value exceeds a significance threshold, the value is propagated to the next layer.

### 3.2. Frame alignment

Robust frame alignment (or video stabilization) is a fundamental requirement for MotionDeltaCNN to achieve high coherence across consecutive frames. For best alignment between two frames in a 3D space, we use homography matrices which support 8 degrees of freedom. Homography matrices align two images in 3D to match a selected set of key features of the initial frame - typically the static background.

We embed the image in a grid-aligned frame to ensure a pixel-perfect downscale to all layers. For example, in HRNet [30], the highest resolution feature map spans 384x384 pixels, whereas the lowest resolution feature map spans only 12x12 pixels, resulting in a scaling factor of 32x32. To ensure that all pixels align on all scaling levels, the input to HRNet must be aligned onto a grid of 32x32 pixel tiles. *E.g.*, if a frame has a 20-pixel horizontal offset relative to the first frame, we allocate 32 additional pixels, paste the original frame into the grid-aligned frame and set the 20 left-most pixels as well as the 12 right-most pixels to zero.

### 3.3. Spherical buffers

MotionDeltaCNN enables support for moving cameras by introducing 2D ring buffers, *spherical buffers*. These buffers align previously processed pixels with pixels of the current frame by translating feature map coordinates to buffer coordinates. Pixel coordinates exceeding image borders are wrapped around the buffer, *i.e.*, mapped to the opposite border using the modulo operator. This enables the reuse of previous results for camera pans without increasing the memory overhead over DeltaCNN (see Figure 3). Our buffers support 2D offsets as well as 2D frame scales relative to the initial frame. Frame scales can be helpful when only a part of the image is updated in the current frame - for example, when a frame is cropped to the bounding box of a region of interest. Tile offset indices are provided during inference to align features in buffers with the current input. By multiplying tile offset indices with a layer’s tile size (in the example above 32x32 pixels in highest resolution feature maps, 1x1 pixel in the lowest resolution), we get the pixel offset coordinates for buffer access in non-linear layers.

### 3.4. Dynamic initialization

When the camera pans over a previously unseen area, new tiles are allocated in all buffers before inferring the frame. A new tile is allocated by deleting a previously stored tile at the desired location and resetting respective values to zero. In doing so, we lose information about the accumulated biases inferred in the initial frame. We compensate this by adding the biases onto reset regions of the Delta feature map during inference. Alternatively, layers with biases (*e.g.*, convolution and batch normalization) that are directly followed by activation layers can initialize the activation layer’s

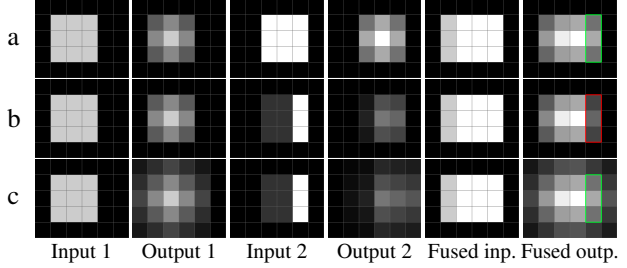


Figure 3. Padded convolutions (c) enable buffer growth over previously unseen regions without artifacts. In this example, we apply a 3x3 average filter on the input. Row a: standard convolution without padding - only the 3x3 pixels containing actual values are processed. The fused output is generated by processing all 4x3 pixels at once. Row b: MotionDeltaCNN without padding - only the Delta of the current 3x3 pixels is processed - newly unveiled pixels lack knowledge of their neighboring pixels’ accumulated values. The fused output does not match that of row a in the newly added column. Row c: MotionDeltaCNN with padding - by processing all pixels that are affected by the current input, newly unveiled pixels include all accumulated values of their neighbors. The fused output of row c matches that of row a for the newly added column.

truncated values buffer with the bias. This way, the bias is implicitly added during the activation/truncation step and does not add additional overhead during inference.

### 3.5. Padded convolutions

After the initial frame, MotionDeltaCNN propagates only Delta updates for the remaining sequence. This becomes a problem when the camera pans, as the CNN input of the new frame contains a mix of Delta updates of previously processed pixels and the actual color values of newly unveiled pixels (which again is the Delta over the previously zero-valued region). This creates inconsistencies when performing the convolution on pixels along the border between Delta values and actual color values. Pixels that were not processed before can only access the current Delta values of their neighbors and therefore lack the information of the accumulated pixel updates from previous frames (see Figure 3). MotionDeltaCNN solves this issue by increasing the padding of convolutional layers to include all pixels that are affected by the current input. This leads to an increase in output size compared to the input when the kernel size is larger than 1x1. For example, with a 64x64 pixel input, and a kernel of size 3x3, we apply an input padding of 2x2 pixels to include all affected pixels, resulting in a 66x66 pixel output. With modern CNNs consisting of hundreds of convolutional layers, a growing feature map would quickly become a problem. We prevent the feature maps from growing indefinitely throughout the network, by storing these *dilated* pixels in buffers for later - and cropping the feature map to its original shape. Since MotionDeltaCNN already



uses truncated values buffers for storing values that were not yet propagated through the activation layer, we only need to increase the size of the buffer slightly to include the *dilated* values and accumulate them there for later use. This allows us to fuse new image regions from all 4 directions seamlessly at the cost of memory and compute overhead for the *dilated* border pixels. Since most convolutions use kernels of size 3x3 and 1x1, however, the overhead is typically low.

### 3.6. Buffer management

We use a buffer manager that is responsible for: keeping track of each tile’s state, allocating new regions in the spherical buffer, initializing newly allocated tiles and adding biases to feature maps during inference. As mentioned before, spherical buffers wrap coordinates around image borders to allow for infinite panning. One downside of this approach is that when borders grow in one direction, we overwrite the *dilated* pixels stored for growing in the opposite direction (see Figure 4). Restoring *dilated* pixels is non-trivial and would require inferring the negative accumulated values of the deleted tiles - which adds high overhead. Instead, we simply delete the *dilated* pixels and restrict the growth into the opposite direction. Once the camera moves back over a restricted region, all buffers are reset entirely, and the current frame has to be inferred densely - becoming the new reference until the next buffer reset. Restoring the truncated values by only resetting the tiles next to the invalid truncated values does not work, as they would again lack valid truncated values required for seamless attachment to persistent tiles. While a full reset reduces the reuse of previously processed features, in our evaluations, the number of resets is fairly small as camera pans typically last many frames without changing directions. Our buffer manager stores for each tile of the grid the currently held global coordinates and the directions in which the growth is restricted. Every time the camera moves, the buffer manager checks whether the tiles already hold a value from the corresponding coordinates. If not, it resets the respective tiles if possible or requests a buffer reset if growth is restricted.

### 3.7. Maximum Pooling

In the original DeltaCNN implementation, maximum pooling layers process the result for newly accumulated inputs and for previously accumulated inputs, which is then subtracted to obtain the Delta output of the layer. In MotionDeltaCNN, this approach does not work anymore as soon as regions inside the accumulated input values buffer are reset to zero. When the pooling kernel accesses a pixel’s neighboring pixels, with some of them reset and others retained from previous frames, the output for the previous frame cannot be processed correctly anymore - leading to incorrect Delta values. We solve this using an additional buffer storing the previous output of a pixel. Since the Delta value is always

relative to the previous output, storing it implicitly solves the dependency on neighboring pixel states. Each pixel was either reset itself in the current frame - in this case, we process the Delta against a zero reference - or it was retained from previous frames - in which case we process the Delta against the previous output.

### 3.8. Optimizations

While the above-mentioned features can already lead to a large speedup in moving camera scenarios, the speedup can be increased significantly with some small optimizations. For the DAVIS 2017 dataset [27], we noticed strong salt-and-pepper style noise in the update masks. Since video stabilization is not perfect, some pixels align incorrectly, especially in high frequency details like leaves of a tree. This leads to a strong color change for some isolated pixels in the image, resulting in a large compute overhead when processing the image in tiles. We mitigate this issue using region-of-interest (ROI) focused sensing and noise suppression. When we know the ROI from previous frames, *e.g.*, in the case of object detection or object segmentation, we can increase the sensitivity around these regions and decrease the sensitivity further away. Additionally, we suppress noise coming from imperfect image alignment by downscaling the Delta, processing which pixels exceed the thresholds and suppressing single pixel updates using average pooling. Overall, these steps lead to a significant speedup with only minor impact on accuracy (see Figure 5).

Furthermore, the number of buffers can be reduced by disabling truncation on selected activation layers. For example, the DenseNet [14] backbone of BMVOS [6] consists mainly of pairs of 3x3 and 1x1 convolutions. In this network, we only truncate in the activation layer following a 3x3 convolution in which updates are dilated. This way, every second activation layer needs only an accumulated values buffer - saving memory at the cost of slightly higher update rates.

## 4. Evaluation

We evaluate MotionDeltaCNN in two scenarios: a) using video stabilization to align subsequent frames with moving cameras and b) using bounding boxes in a static camera scenario to infer only regions of interest while retaining out-of-interest features from previous frames.

**Video Object Segmentation** In task a), we evaluate the video object segmentation model BMVOS [6] on the DAVIS 2017 dataset [27]. BMVOS uses the DenseNet [14] backend for feature encoding, the most computationally expensive part of the model. We use weights pretrained on the DAVIS dataset, which were provided by the authors of BMVOS. The DAVIS 2017 dataset consists of a set of sequences with one or more segmented objects of which the masks are provided only for the first frame - and the model needs to paint the segmentation mask for the remaining frames in the video.

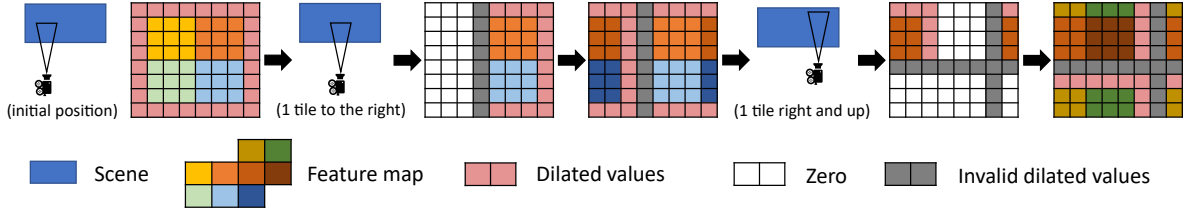


Figure 4. Our spherical buffers use tile offsets to access the correct locations in caches for the current input. When the camera pans over unseen regions, unused regions in the buffer are reset and allocated for the newly unveiled pixels. This process deletes the truncated *dilated* values stored on the border of the tiles which allow new regions to be attached seamlessly. When the camera pans back over an invalid dilated value, the buffers have to be reset entirely, triggering a dense inference of the next frame.

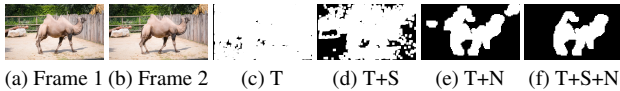


Figure 5. We increase update sparsity using noise suppression and region of interest scaling.  $T$  is the original truncation implementation used in DeltaCNN. Scaling the Delta further away from the region of interest ( $T + S$ ), we achieve a slightly higher sparsity. Using noise suppression ( $T + N$ ) to eliminate single pixel updates increased the sparsity even further. Combining scaling and noise suppression ( $T + S + N$ ) achieves the highest sparsity, capturing only the most important updates of the moving camel. Note that in all cases, we dilate the resulting update mask by 10 pixels; explaining the nearly dense mask in case  $T$  in this example.

Most of the videos are recorded using moving cameras, and are therefore well suited for evaluating MotionDeltaCNN. The DAVIS 2017 dataset does not provide camera extrinsics. Instead, we use OpenCV [2] to estimate homography matrices between two consecutive frames. This simplistic method fails in some cases, *e.g.*, when it does not find good features due to motion blur or with motion parallax. We see the tasks of video stabilization as orthogonal and therefore only evaluate on the set of videos (14 sequences) for which this simple video stabilization approach works reliably.

In video object segmentation, the segmentation mask from the previous frame can be used to suppress noise in the upcoming frame. We use this mask to lower the update sensitivity further away from the ROI - leading to an increase in sparsity. We dilate the previous mask multiple times using maximum pooling with different kernel sizes (10, 20, 40) and compute the average pixel values of the three masks  $m$ . The image Delta is then scaled using a factor of  $0.4 + 0.6 * m$  before comparing it against the truncation threshold.

The thresholds are auto-tuned on a sequence from the training dataset (tractor-sand) using a threshold of 0.02 as a starting point for all layers but the first which uses 0.15 and an update mask dilation of 10 pixels (a single pixel update would be dilated over 21x21 pixels). We do not use the same, sensitive thresholds for DeltaCNN since they lead to dense updates nearly every frame due to the lack of image align-

ment. Instead, we increase the threshold of the first layer to 0.2 and auto tune the remaining thresholds on the same sequence without frame alignment. This leads to a slightly lower accuracy for DeltaCNN than for MotionDeltaCNN. We deliberately target a lower accuracy when tuning the thresholds for DeltaCNN since we aim to show that we outperform DeltaCNN even when they are allowed to truncate updates more aggressively. The auto-tuning procedure is implemented as an iterative front-to-back process as described in DeltaCNN [26].

**Human Pose Estimation** In task b), we perform human pose estimation using *HRNet* on the *Human3.6M* dataset. Human3.6M uses static cameras and is recorded in a static studio with only a single moving actor in the room. We use this dataset to evaluate a second scenario for MotionDeltaCNN: top-down pose estimation. With top-down pose estimation, humans in the scene are detected first, and then the pose is predicted for each detected human. Each bounding box is cropped and inferred individually - estimating one set of joints per person. Since Human3.6M provides per frame bounding boxes of the actors as part of their labels, we omit the step of detecting humans in the scene. We snap the given bounding boxes onto a 32x32 pixel grid and then increase them by 32 pixels on each side where possible. The increased bounding boxes ensure that joint positions are not too close to image borders, as this could negatively impact prediction accuracy. We use the same weights and thresholds as were used in the DeltaCNN paper and evaluate on the same data subset (Subject S11).

Both scenarios are compared against dense inference of cuDNN and against the original DeltaCNN without moving camera support. In HRNet, we only measure model inference time, without the overhead of post-processing or accuracy evaluation. The input shape is 384x384 with a tile size of 32x32 pixels unless stated otherwise. In case of BMVOS, we only measure the duration of the feature encoding model to better highlight the difference of pure CNN inference speeds. For this evaluation, the camera input is embedded into a frame of shape  $W \times 480$  pixels, where  $W$  depends on the aspect ratio of the video (typically 864px)



Figure 6. Two example sequences processed using MotionDeltaCNN. Row a shows the aligned and cropped input. Row b visualizes the Delta between the aligned input and the previous input in row c. Row d visualizes the update mask with white pixels indicating an update.

and is aligned onto a grid with a tile size of 48x48 pixels.

**Hardware** We conduct our evaluations on two GPUs: Nvidia GTX 1080 Ti and Nvidia RTX 3090 with 3584/10496 CUDA cores and 11GB/24GB of VRAM respectively. The evaluations are performed using 32-bit precision, but our approach can be applied to other data types as well.

## 5. Results

We evaluate speedup and accuracy of MotionDeltaCNN compared to DeltaCNN without explicit moving camera support as well as the dense cuDNN backend. In this section, we report the differences on the GTX 1080 Ti - for results on the RTX 3090, please see the respective tables.

**Video Object Segmentation** MotionDeltaCNN outperforms state-of-the-art backends in sparse mode by a margin of up to 100% over the cuDNN baseline (see Table 1). The DAVIS 2017 dataset consists mainly of videos with large bounding boxes and often fast camera motion, leading to a high average update rate of 29%.

Excluding videos without camera motion highlights the relative speedup over DeltaCNN without moving camera support with +85% speedup over cuDNN instead of +8%.

MotionDeltaCNN, like DeltaCNN, requires larger workloads with more powerful hardware to show speedups. With 10.496 cores in a RTX 3090, small batch sizes typically do not fully utilize the available hardware resources in most layers - skipping some tiles in this scenario does not affect the overall performance unless all tiles can be skipped altogether. By increasing the batch size, we can fully utilize the GPU - cores that skip a tile can immediately continue processing the next tile, leading to an overall speedup.

Over the 990 frames in the DAVIS dataset, we had to reset the buffers 9 times because of cameras panning over invalid truncated values. This low number of resets has only a small impact on the overall performance.

**Human Pose Estimation** MotionDeltaCNN can outper-

form cuDNN by up to 11x in the case of HRNet (see Table 2). Please note that the frame rate of cuDNN is 30% lower than in the DeltaCNN paper since we enforced the use of 32-bit multiplications in all layers - the same accuracy that we also use in our implementation. Furthermore, the accuracies do not match since we always use the full, uncropped images as input. The high sparsity in the Human3.6M dataset together with the efficient implementation allows us to accelerate inference significantly. Compared to DeltaCNN, which does not support varying resolution input or moving cameras, we were able to achieve 13% higher frame rates with similar accuracy. We level the playing field in comparisons against the dense cuDNN backend by inferring the same cropped images that we use as input for MotionDeltaCNN. Still, we outperform cuDNN by up to 3.9x, and achieve a speedup of up to 3.2x over dense DeltaCNN with full resolution input. For Human3.6M, we know that the actors never cover the entire frame at once. We use this knowledge to lower the size of the buffers by 25% on each axis - reducing the memory footprint of buffers by 44% in total. These savings allow us to increase the batch size even further. When fully utilizing all available memory with an increased batch size, we achieve frame rates up to 3.9x over the cropped cuDNN baseline and 37% over DeltaCNN.

## 6. Discussion

Our evaluations prove that MotionDeltaCNN can accelerate CNN video inference with moving cameras. We achieve speedups with moving camera input where existing sparse methods fail to outperform the dense reference. However, our evaluation also shows that freely moving cameras, especially when combined with dense updates as in the DAVIS dataset, lead to a much smaller speedup than the static camera setup with sparse motion in Human3.6M. Furthermore, the additional padding increases memory and compute overhead over DeltaCNN.

**Receptive Field** While MotionDeltaCNN does achieve



Videos	Backend	IoU	GFLOPs	GTX 1080 Ti b=1		GTX 1080 Ti b=4		RTX 3090 b=1		RTX 3090 b=12	
				FPS	speedup	FPS	speedup	FPS	speedup	FPS	speedup
All	cuDNN	76.85	22.1	30.7	1.0	40.9	1.0	45.4	1.0	103	1.0
	DeltaCNN (dense)	76.85	22.1	35.0	1.14	41.2	1.01	66.5	1.46	100	0.97
	MotionDeltaCNN (dense)	76.76	22.6	33.5	1.09	40.3	0.99	57.7	1.27	93.6	0.91
	DeltaCNN (sparse)	76.18	15.5	42.5	1.38	51.4	1.26	<b>70.0</b>	<b>1.54</b>	125	1.21
	<b>MotionDeltaCNN (sparse)</b>	76.32	<b>6.8</b>	<b>54.8</b>	<b>1.79</b>	<b>81.9</b>	<b>2.00</b>	65.2	1.44	<b>215</b>	<b>2.1</b>
Moving	cuDNN	79.59	22.1	30.7	1.0	40.9	1.0	45.4	1.0	103	1.0
	DeltaCNN (sparse)	79.38	18.8	38.2	1.24	44.1	1.08	<b>70.2</b>	<b>1.55</b>	106	1.03
	<b>MotionDeltaCNN (sparse)</b>	79.43	<b>7.3</b>	<b>52.3</b>	<b>1.70</b>	<b>75.1</b>	<b>1.84</b>	65.0	1.43	<b>201</b>	<b>1.95</b>

Table 1. Results for the task of video object segmentation using BMVOS on the DAVIS dataset. We track only the DenseNet backend for evaluating frames per second (FPS). For accuracy benchmarks, the remaining network is processed densely. GFLOPs are reported as average over the test set. Both devices are evaluated with a batch size  $b$  of one, and the maximum batch size each device can hold in memory.

Backend	PCKh@0.5	PCKh@0.2	GFLOPs	GTX 1080 Ti b=1		GTX 1080 Ti b=16		RTX 3090 b=1		RTX 3090 b=40	
				FPS	speedup	FPS	speedup	FPS	speedup	FPS	speedup
cuDNN	96.03%	83.33%	47.1	22.5	1.0	24.8	1.0	12.3	1.0	69.6	1.0
DeltaCNN (dense)				24.2	1.08	41.3	1.7	26.0	2.1	95.8	1.4
ours (dense)	96.00%	83.32%	17.7	32.5	1.44	91.4	3.7	22.0	1.8	232	3.3
cuDNN (cropped)	95.92%	83.11%	13.3	24.0	1.07	71.0	2.9	11.8	1.0	209	3.0
DeltaCNN (sparse)	95.95%	82.31%	3.55	<b>44.9</b>	<b>2.0</b>	202	8.1	<b>26.2</b>	<b>2.1</b>	547	7.9
<b>MotionDeltaCNN (sparse)</b>	95.95%	82.33%	3.45	41.2	1.83	228	9.2	22.6	1.8	584	8.4
<b>MotionDeltaCNN (sparse †)</b>	95.93%	82.22%	<b>3.44</b>	42.5	1.89	<b>276</b>	<b>11.1</b>	22.5	1.8	<b>691</b>	<b>9.9</b>

Table 2. Speed and accuracy comparisons of different CNN backends used for pose estimation on the Human3.6M dataset. The same set of auto-tuned thresholds for update truncation is used for all devices and batch sizes  $b$ . † limits the size of the input from 384x384 to 288x288 pixels - freeing up 44% of the memory used for buffers. The freed-up memory is used to increase the batch size to fully utilize the available VRAM ( $b=28$  on 1080 Ti and  $b=66$  on 3090). cuDNN cropped uses the same, cropped input as ours, instead of the full camera input.

outputs comparable to standard CNN inference, it should be noted that even in dense mode, the results are not identical. This can be observed in Figure 3 where the fused output of MotionDeltaCNN matches the result using the fused input in row a, which is different to output 2, the output with conventional inference. Since we do not actively propagate inverted accumulated values once a previously processed region gets out of view, the receptive field of later layers, also for pixels inside the current view, still contains some information from that now unseen area. This can have positive and negative effects alike. These features are outdated and might not be valid anymore. At the same time, some out-of-view features can help to make better predictions on the currently visible input. We see this effect in the case of Human3.6M, where MotionDeltaCNN achieves a higher accuracy than cuDNN on the same cropped inputs (see Table 2).

**Limitations** One of the main limitations of our approach is its dependency on robust video stabilization. Our experiments with the DAVIS dataset showed that simple video stabilization techniques can break when blur or parallax is involved, or when it fails to find robust features. Parallax can greatly reduce the gains of our method, even when the scene

itself is mostly static. When foreground and background layers move at different speeds, frames can only be properly aligned to stabilize one of these layers - leading to dense updates in layers moving at different speeds.

MotionDeltaCNN also comes with the trade-off between buffer overallocation and losing information by cropping the input to match the shape of the buffer. In our evaluations, when the camera zooms or rotates around the forward axis (*roll*), the aligned input can exceed the size of the buffers, and therefore requires slight cropping to fit into the target shape (see Figure 6). Alternatively, the buffers could also be increased to allow for larger inputs in upcoming frames - at the cost of higher memory consumption.

## 7. Conclusion

We propose MotionDeltaCNN, an extension to the sparse video CNN framework DeltaCNN adding support for moving camera input. To the best of our knowledge, we are the first to propose a solution for moving cameras with sparse inference. MotionDeltaCNN uses spherical buffers, padded convolutions and dynamic initialization of newly unveiled regions to support combining previously processed pixels



and newly unveiled pixels together with high sparsity. We test our approach in practice by implementing all kernels natively on the GPU to evaluate the real-world performance with modern hardware. Our experiments show that we outperform existing methods by up to 90% on moving camera input and that MotionDeltaCNN can also be beneficial to lower the memory footprint in static camera scenarios.

## References

- [1] Udari De Alwis and Massimo Alioto. TempDiff: Temporal Difference-Based Feature Map-Level Sparsity Induction in CNNs with <4% Memory Overhead. *2021 IEEE 3rd International Conference on Artificial Intelligence Circuits and Systems, AICAS 2021*, pages 1–4, Jun 2021. **1**
- [2] G. Bradski. The OpenCV Library. *Dr. Dobb's Journal of Software Tools*, 2000. **6**
- [3] Lukas Cavigelli and Luca Benini. CBInfer: Exploiting Frame-to-Frame Locality for Faster Convolutional Network Inference on Video Streams. *IEEE Transactions on Circuits and Systems for Video Technology*, 30(5):1451–1465, May 2020. **1, 2**
- [4] Yunji Chen, Tianshi Chen, Zhiwei Xu, Ninghui Sun, and Olivier Temam. DianNao family: Energy-efficient hardware accelerators for machine learning. *Communications of the ACM*, 59(11):105–112, 2016. **1**
- [5] Yunji Chen, Tao Luo, Shaoli Liu, Shijin Zhang, Liqiang He, Jia Wang, Ling Li, Tianshi Chen, Zhiwei Xu, Ninghui Sun, and Olivier Temam. DaDianNao: A Machine-Learning Supercomputer. *Proceedings of the Annual International Symposium on Microarchitecture, MICRO*, 2015-January:609–622, Jan 2015. **1**
- [6] Suhwan Cho, Heansung Lee, Minjung Kim, Sungjun Jang, and Sangyoun Lee. Pixel-Level Bijective Matching for Video Object Segmentation. *Proceedings - 2022 IEEE/CVF Winter Conference on Applications of Computer Vision, WACV 2022*, pages 1453–1462, 2022. **5**
- [7] Matthew Dutson, Yin Li, and Mohit Gupta. Event neural networks. 2021. **1, 3**
- [8] Zhipeng Fan, Jun Liu, and Yao Wang. Adaptive Computationally Efficient Network for Monocular 3D Hand Pose Estimation. Technical report, 2020. **1**
- [9] Benjamin Graham, Martin Engelcke, and Laurens Van Der Maaten. 3D Semantic Segmentation with Submanifold Sparse Convolutional Networks. *Proceedings of the IEEE Computer Society Conference on Computer Vision and Pattern Recognition*, pages 9224–9232, Nov 2018. **3**
- [10] Amirhossein Habibian, Davide Abati, Taco S. Cohen, and Babak Ehteshami Bejnordi. Skip-Convolutions for Efficient Video Processing. In *Proceedings of the IEEE/CVF Conference on Computer Vision and Pattern Recognition (CVPR)*, pages 2695–2704, Jun 2021. **1, 2**
- [11] Amirhossein Habibian, Haitam Ben Yahia, Davide Abati, Efstratios Gavves, and Fatih Porikli. Delta Distillation for Efficient Video Processing. *arXiv (ECCV sub)*, 2022. **1**
- [12] Song Han, Xingyu Liu, Huizi Mao, Jing Pu, Ardavan Pedram, Mark A. Horowitz, and William J. Dally. EIE: Efficient Inference Engine on Compressed Deep Neural Network. *Proceedings - 2016 43rd International Symposium on Computer Architecture, ISCA 2016*, pages 243–254, 2016. **1**
- [13] Song Han, Jeff Pool, John Tran, and William J. Dally. Learning both weights and connections for efficient neural networks. *Advances in Neural Information Processing Systems*, 2015-January:1135–1143, 2015. **1**
- [14] Gao Huang, Zhuang Liu, Laurens Van Der Maaten, and Kilian Q. Weinberger. Densely connected convolutional networks. *Proceedings - 30th IEEE Conference on Computer Vision and Pattern Recognition, CVPR 2017*, 2017-January:2261–2269, 2017. **5**
- [15] Itay Hubara, Matthieu Courbariaux, Daniel Soudry, Ran El-Yaniv, and Yoshua Bengio. Quantized neural networks: Training neural networks with low precision weights and activations. *Journal of Machine Learning Research*, 18:1–30, 2018. **1**
- [16] Samvit Jain, Xin Wang, and Joseph E. Gonzalez. Accel: A corrective fusion network for efficient semantic segmentation on video. *Proceedings of the IEEE Computer Society Conference on Computer Vision and Pattern Recognition*, 2019-June:8858–8867, Jun 2019. **1**
- [17] Alex Krizhevsky, Ilya Sutskever, and Geoffrey E Hinton. ImageNet classification with deep convolutional neural networks. In F. Pereira, C.J. Burges, L. Bottou, and K.Q. Weinberger, editors, *Advances in Neural Information Processing Systems*, volume 25. Curran Associates, Inc., 2012. **1**
- [18] CUN Le. Optimal brain damage. *Advances in Neural Information Processing Systems*, 2:598–605, 1990. **1**
- [19] Yule Li, Jianping Shi, and Dahua Lin. Low-Latency Video Semantic Segmentation. *Proceedings of the IEEE Computer Society Conference on Computer Vision and Pattern Recognition*, pages 5997–6005, 2018. **1**
- [20] Feng Liang, Ting-Wu Chin, Yang Zhou, and Diana Marculescu. Ant: Adapt network across time for efficient video processing. In *Proceedings of the IEEE/CVF Conference on Computer Vision and Pattern Recognition (CVPR) Workshops*, pages 2603–2608, June 2022. **1**
- [21] Darryl D. Lin, Sachin S. Talathi, and V. Sreekanth Anna-pureddy. Fixed point quantization of deep convolutional networks. *33rd International Conference on Machine Learning, ICML 2016*, 6:4166–4175, 2016. **1**
- [22] Leyao Liu, Tian Zheng, Yun-jou Lin, Kai Ni, and Lu Fang. INS-Conv : Incremental Sparse Convolution for Online 3D Segmentation. *Cvpr*, pages 18975–18984, 2022. **3**
- [23] Bert Moons, Koen Goetschalckx, Nick Van Berckelaer, and Marian Verhelst. Minimum energy quantized neural networks. *Conference Record of 51st Asilomar Conference on Signals, Systems and Computers, ACSSC 2017*, 2017-October:1921–1925, Apr 2018. **1**
- [24] Xuecheng Nie, Yuncheng Li, Linjie Luo, Ning Zhang, and Jiashi Feng. Dynamic kernel distillation for efficient pose estimation in videos. *Proceedings of the IEEE International Conference on Computer Vision*, 2019-October:6941–6949, Oct 2019. **1**
- [25] Bowen Pan, Wuwei Lin, Xiaolin Fang, Chaoqin Huang, Bolei Zhou, and Cewu Lu. Recurrent Residual Module for Fast Inference in Videos. Technical report, 2018. **1, 2**

- [26] Mathias Parger, Chengcheng Tang, Christopher D. Twigg, Cem Keskin, Robert Wang, and Markus Steinberger. Deltacnn: End-to-end cnn inference of sparse frame differences in videos. In *Proceedings of the IEEE/CVF Conference on Computer Vision and Pattern Recognition (CVPR)*, pages 12497–12506, June 2022. [1](#), [2](#), [6](#)
- [27] Jordi Pont-Tuset, Federico Perazzi, Sergi Caelles, Pablo Arbeláez, Alexander Sorkine-Hornung, and Luc Van Gool. The 2017 davis challenge on video object segmentation. *arXiv:1704.00675*, 2017. [5](#)
- [28] Evan Shelhamer, Kate Rakelly, Judy Hoffman, and Trevor Darrell. Clockwork convnets for video semantic segmentation. *Lecture Notes in Computer Science (including subseries Lecture Notes in Artificial Intelligence and Lecture Notes in Bioinformatics)*, 9915 LNCS:852–868, 2016. [1](#)
- [29] Laurent Sifre and Stéphane Mallat. PhD Thesis, Ecole Polytechnique, CMAP Rigid-Motion Scattering For Image Classification. 2014. [1](#)
- [30] Ke Sun, Bin Xiao, Dong Liu, and Jingdong Wang. Deep high-resolution representation learning for human pose estimation. *Proceedings of the IEEE Computer Society Conference on Computer Vision and Pattern Recognition*, 2019-June:5686–5696, 2019. [4](#)
- [31] Mingxing Tan and Quoc V. Le. EfficientNet: Rethinking model scaling for convolutional neural networks. Technical report, 2019. [1](#)
- [32] Xizhou Zhu, Jifeng Dai, Lu Yuan, and Yichen Wei. Towards High Performance Video Object Detection. *Proceedings of the IEEE Computer Society Conference on Computer Vision and Pattern Recognition*, pages 7210–7218, 2018. [1](#)
- [33] Xizhou Zhu, Yuwen Xiong, Jifeng Dai, Lu Yuan, and Yichen Wei. Deep feature flow for video recognition. *Proceedings - 30th IEEE Conference on Computer Vision and Pattern Recognition, CVPR 2017*, 2017-January:4141–4150, 2017. [1](#)